

# Geostatistical-Inspired Metamodeling and Optimization of Nano-CMOS Circuits

Oghenekarho Okobiah<sup>1</sup>, Saraju P. Mohanty<sup>2</sup>, and Elias Kougianos<sup>3</sup>  
NanoSystem Design Laboratory (NSDL, <http://nsdl.cse.unt.edu>)  
University of North Texas, Denton, TX 76207, USA.  
Email ID: oo0032@unt.edu<sup>1</sup>, saraju.mohanty@unt.edu<sup>2</sup>, and eliask@unt.edu<sup>3</sup>

**Abstract**—With the continuous progression of semiconductor technology, nanoscale effects have become a persistent issue in the design of analog/mixed-signal (AMS) circuits. The cost of exploration and optimization of the design space increases to infeasible levels with conventional design methodologies. Different modeling techniques to reduce the cost of design exploration, while ensuring the accuracy of such models, have been introduced and continue to be a research problem. In this paper, a geostatistical inspired metamodeling and optimization technique is presented for fast and accurate design optimization of nano-CMOS circuits. The proposed design methodology incorporates a simple Kriging based metamodel which efficiently and accurately predicts design performance. The metamodel (instead of the circuit netlist) is subjected to a Gravitational Search Algorithm for optimization. This design methodology is applicable to AMS circuits and is illustrated with the optimization of power consumption of a 45nm CMOS thermal sensor. The method improves the power performance of the thermal sensor by 36.9% while reducing the design optimization time by 90% even with 6 design parameters.

**Keywords**—Nano-CMOS, Geostatistics, Kriging methods, Gravitational search algorithm, AMS design flow.

## I. INTRODUCTION

The demand for smaller, portable, more powerful and efficient consumer electronics continues to drive the aggressive scaling of semiconductor technologies. However, as the scaling continues, designers are not only faced with the challenges of subthreshold leakage and power density, but also with the effects of process variation. Accurate and exhaustive simulation of design models has become considerably computationally intensive and time consuming due to the increase of design and process parameters to be considered. Current techniques used to reduce simulation time include the use of metamodeling functions [1], [2], [3], [4] and performance estimation through Monte Carlo simulations.

Metamodeling functions are approximations of performance objectives of the simulated design model with respect to design parameters [1]. Low-order polynomial functions and artificial neural network models are common metamodeling techniques. The accuracy and efficiency of a metamodel depends on the technique used in creating it [4]. For instance, metamodels based on low-order polynomial regression functions deliver accurate circuit descriptions, but are not efficient when used for global optimization [2]. When predicting the objective function, the regression models assume the effects of process variation are purely random and approximate the error equally

across the design space. However, in nano-CMOS technology, this is not the case. The effects of process variation are not purely random, but they are also strongly correlated. Kriging based metamodels which are based on geostatistical means, take into account by their weighting system the correlation effects between the design parameters. Kriging metamodeling techniques which account for the correlation effects of process variation, provide a robust metamodel which is process variation and yield aware, thus giving designers a greater control over the design parameters.

With available design metamodels, designers also face the challenge of effectively exploring the design space. In high dimensional parameter designs, as is the case with nano-CMOS circuits, exhaustive search space optimization techniques are unrealistic as the search space increases exponentially with problem size [5]. Different optimization algorithms utilized for circuit design optimization include genetic algorithms, swarm algorithms, simulated annealing, tabu search and geometric programming [6], [7], [4]. To mitigate the above issues, in the current paper, **a novel AMS circuit optimization methodology is proposed** which incorporates a geostatistical-inspired metamodel technique with a gravitational search algorithm.

The rest of this paper is organized as follows. The major contributions of this paper are outlined in Section II. A summary review of related research is presented in Section III. In Section IV, a brief overview of Kriging modeling and in particular simple Kriging is discussed. In Section V, the background and theory of the Gravitational Search Algorithm is described. The overall proposed design flow is presented in Section VI. In Section VII, an illustration of the design flow is presented on the design optimization of a 45 nm thermal sensor. The conclusions and future research directions are presented in Section VIII.

## II. NOVEL CONTRIBUTIONS OF THIS PAPER

In this paper, the use of geostatistical methods is introduced in a design flow methodology for mixed-signal circuit design optimization due to their capability of accounting for correlation effects of the design parameters to produce robust and accurate metamodels. A gravitational search algorithm is proposed to employ both exploitative and explorative aspects of population based algorithms effectively using gravity rules. A case study circuit, a 45nm thermal sensor is used to illustrate the performance of the proposed methodology. With

the proposed methodology, the optimization of the power consumption with the thermal sensitivity as a design constraint is illustrated. Optimizing the power consumption in thermal sensor circuits is crucial to the operation of the circuit, as higher power dissipation leads to increased temperatures resulting in performance degradation. The **summary of the novel contributions of the current paper** to the state-of-the-art are the following:

- 1) An AMS design flow methodology incorporating simple Kriging based metamodels.
- 2) Application of the Gravitational Search Algorithm (GSA) for AMS circuit optimization.
- 3) A 45 nm thermal sensor circuit power minimization with the thermal sensitivity as a design constraint.

### III. RELATED PRIOR RESEARCH

In [8], [9], a study and comparison of metamodeling techniques including polynomial regression, artificial neural networks (ANN), radial basis Low-order polynomial regression techniques provide fast and efficient accurate metamodels but do not perform well in global optimization problems [2], [10]. In [7], a technique which applies geometric programming to polynomial equations deduced from circuit designs improves global optimizations. Artificial neural networks are used in [10], [11] for the metamodeling of discrete stochastic systems. In [12], [13], Kriging techniques have also been used for circuit design.

Design optimization remains a prominent issue especially for analog and mixed-signal circuits. In [6], a comparison of simulated annealing, genetic algorithm and gradient based algorithm is presented. In [14], a swarm algorithm technique using orthogonal optimization techniques is presented. Fast optimization algorithms based on artificial bee colonies is presented in [15].

The optimization of thermal sensor design is also a well researched topic. The need for low power designs without degrading the accuracy of temperature estimation poses a problem. A thermal sensor design based on differential ring oscillators (DRO) was proposed in [16]. In [17], a methodology which incorporates statistical techniques into the design process aids the estimation of temperature effects on the circuit. In [18], a design which uses a reference transistor independent of ambient temperature to reduce its effects on accuracy is proposed.

### IV. PROPOSED SIMPLE KRIGING METAMODELING

The simple Kriging metamodel generation flow is presented in Fig. 1. Latin Hypercube Sampling (LHS) is used to accurately obtain the sample points from the complex design space to be used for the Kriging metamodel generation. LHS is selected to cover all input dimensions simultaneously and thus improving on the variance over Monte Carlo distributions. In [4], a comparison of sampling techniques show that LHS generates more accurate models over random sampling points.

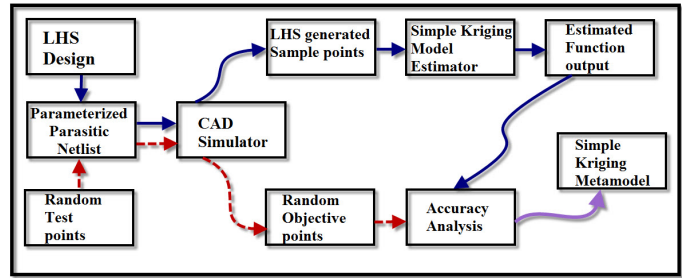


Fig. 1. The proposed simple Kriging metamodel generation flow.

The use of Kriging was proposed in [19] as a stochastic approach to compensate for the deterministic nature of computer simulations. Kriging techniques use weighted averages which are unique to each predicted point. The weights are a function of the correlation between the sampled data points and the point to be estimated. The general expression of a Kriging model is as follows:

$$y(\mathbf{x}_0) = \sum_{j=1}^L \lambda_j B_j(\mathbf{x}) + z(\mathbf{x}), \quad (1)$$

where  $y(\mathbf{x}_0)$  is a stochastic function which predicts the response at the design point  $(\mathbf{x}_0)$ .  $\{B_j(\mathbf{x}), j = 1, \dots, L\}$  is a specific set of basic functions over the design domain  $D_N$ ,  $\lambda_j$  are fitting coefficients (weights) to be determined and  $z(\mathbf{x})$  is a stochastic process with zero mean and is based on a spatial correlation function called the *variogram*, given by:

$$r(\mathbf{s}, \mathbf{t}) = \text{Corr}(z(\mathbf{s}), z(\mathbf{t})). \quad (2)$$

The variogram is used to derive the Kriging weights,  $\lambda_j$ . The autocorrelation of the design points is characterized by the covariance function [20]. The weights are chosen so that the Kriging variance is minimized.

The **simple Kriging method is used in the current paper**. It assumes a constant and known mean over the global domain. Assuming that there are  $n$  sample points, of variable  $x$ , to predict a new point  $y(x_0)$ , the weights  $\lambda$  are estimated by:

$$\begin{pmatrix} \lambda_1 \\ \vdots \\ \lambda_n \end{pmatrix} = \Gamma^{-1} \begin{pmatrix} \gamma(x_1, x_0) \\ \vdots \\ \gamma(x_n, x_0) \end{pmatrix}. \quad (3)$$

$\Gamma$  is the covariance matrix of the observed points given by:

$$\Gamma = \begin{pmatrix} \gamma(x_1, x_1) & \cdots & \gamma(x_1, x_n) \\ \vdots & \ddots & \vdots \\ \gamma(x_n, x_1) & \cdots & \gamma(x_n, x_n) \end{pmatrix}. \quad (4)$$

Where  $\gamma(x_1, x_2) = E(|z(x_1) - z(x_2)|^2)$ .

A MATLAB toolbox developed for the implementation of Kriging models [21] is used in this paper to predict the output response. It takes in  $n$  sample points with the observed output and parameters to specify the Kriging technique and variogram model along with a set of design points to be predicted. The output is the predicted response with an estimated error.

The generated metamodels must be validated before use for design exploration or optimization. Validation tests ensure the accuracy of the metamodel and are usually done with additional random points through statistical analysis. The metrics Mean Square Error (MSE), Root Mean Square (RMSE) and the correlation coefficient  $R^2$  are used. A lower value for both MSE and RMSE indicate a more accurate model, while a higher  $R^2$  value implies a more accurate model. Sample performance points are produced from SPICE simulations using the LHS generated points.

## V. PROPOSED GRAVITATIONAL SEARCH ALGORITHM

The gravitational search algorithm (GSA) was introduced in 2009 [5] as a new heuristic optimization algorithm based on the newtonian laws of gravity. The proposed GSA algorithm models the search agents as mass objects. Heavier masses correspond to better performing agents (i.e. design points with superior performance objectives.) As agent masses become heavier, they attract other agents towards them by gravity force, hence pulling search agents towards an area with a likely optimal solution. Agents which attract other masses become heavier and move slower, concentrating in a search area with a likely optimal solution while lighter masses are able to move faster exploring other search locations. Assume a system with  $N$  denoting the number of masses (search agents/nodes). The location (design point) of the  $i$ th mass can be expressed in functional form as follows:

$$X_i = (x_i^1, x_i^2, \dots, x_i^d, \dots, x_i^n) \text{ for } i = 1, 2, \dots, N, \quad (5)$$

where  $x_i^d$ , presents the position of the  $i$ th agent in the  $d$ th dimension, and  $n$  is the number of dimensions.

The attractive force on a mass object ‘ $i$ ’ from a mass object ‘ $j$ ’ is given by:

$$F_{ij}^d(t) = G(t) \left( \frac{M_{pi}(t) \times M_{aj}(t)}{R_{ij}(t) + \epsilon} \right) (x_j^d(t) - x_i^d(t)). \quad (6)$$

Where  $M_{aj}$  and  $M_{pi}$  are the active and passive gravitational masses of objects ‘ $j$ ’ and ‘ $i$ ’ respectively,  $G(t)$  is a gravitational constant at time  $t$ , and  $R_{ij}$  is the Euclidean distance between the two objects. The mass of each agent is updated with the following expressions:

$$M_i(t) = \frac{m_i(t)}{\sum_{j=1}^N m_j(t)}, \quad (7)$$

$$m_i(t) = \frac{fit_i(t) - worst(t)}{best(t) - worst(t)}, \quad (8)$$

where  $fit_i(t)$  represents the best solution found in each iteration. Thus, the total force acting on an object is:

$$F_i^d(t) = \sum_{j=1, j \neq i}^N rand_j F_{ij}^d(t), \quad (9)$$

where  $rand_j$  is a random number between 0 and 1. The use of the random number adds a stochastic flavor to the algorithm.

The mass locations which find optimal solutions gradually attract masses with poor performance, effectively increasing

the chances of exploitation but also ensuring exploration of the design space. A convergence of the masses by the heaviest mass presents an optimal solution of the search space. One appealing feature of the GSA is that it is memoryless, it does not need to remember previous best solutions but still guarantees near-optimal solution by virtue of mass acquisition.

The pseudocode of the GSA is shown in Algorithm 1. In the pseudocode, steps 1 - 3 sets up the optimization flow, by setting up the maximum number of iterations and the number of mass agents to use for optimization. Step 4 sets up the location of each of the search nodes with generic masses. Steps 7-14 consist of the main section which analyzes each search node per iteration and updates the mass, velocity and location, reiteratively until an optimal solution is found or the termination criteria met.

---

### Algorithm 1 Proposed Gravitational Search.

---

- 1: Initialize iteration counter:  $counter \leftarrow 0$ .
  - 2: Initialize max iteration  $Max_{iter}$ .
  - 3: Initialize number of search agents  $\eta$  gravity constant  $G$ , and velocity  $\nu$ .
  - 4: Generate  $\eta$  random search nodes (design parameter sets).
  - 5: Consider the objective of interest  $Power_{TS_i}$ .
  - 6:  $counter \leftarrow max\_Iteration$ .
  - 7: **while** ( $counter < Max_{iter}$ ) **do**
  - 8: Evaluate objective of interest ( $Power_{TS_i}$ ) for each search node.
  - 9: Update best and worst solution per function objective.
  - 10: Update the gravity constant  $G$ .
  - 11: Calculate  $M$  and  $a$  for each search node.
  - 12: Update  $\nu$  for each search node.
  - 13: Update search nodes by applying velocity on  $M$ .
  - 14:  $counter \leftarrow counter + 1$ .
  - 15: **end while**
  - 16: **return**  $bestsolution$ .
- 

## VI. OVERALL DESIGN OPTIMIZATION FLOW

The proposed overall design optimization flow is shown in Fig. 2. The design process incorporates a geostatic inspired metamodel parasitic aware design that is optimized using the gravitational search algorithm. The process starts with the designing the circuit schematic to meet design specifications. Once the circuit is complete, a simulation is performed for functional verification, the design is also checked to ensure that it meets specifications. The circuit is redesigned if it does not meet specifications. After the circuit schematic is completed, the physical design is also drawn. Design Rule Check (DRC) and Layout versus Schematic (LVS) is performed on the completed physical design. The parasitic netlist is then fully extracted (R-resistance, L-inductance, C-capacitance, and K-mutual inductance). This parasitic netlist is fully parameterized with the design variables. The output of the physical design is usually degraded by the parasitic effects. The parametrization of the extracted netlist allows for easy and efficient redesign of the layout without having to manually resize the transistors.

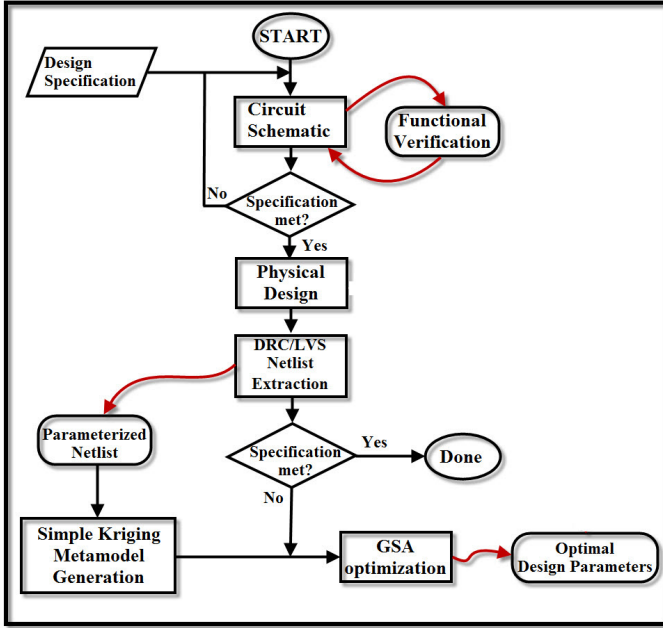


Fig. 2. The proposed overall design optimization flow.

## VII. EXPERIMENTAL RESULTS

An illustration of the proposed design optimization flow is presented with the power optimization of a 45 nm thermal sensor used as a case study circuit. The tools used for the experimental set were the schematic and layout editors on the Cadence Virtuoso platform. MATLAB was used to implement the metamodel generation and optimization algorithm using the MATLAB toolboxes, mGstat [21], and GSA [5].

### A. The Case Study Circuit: 45nm Thermal Sensor

The thermal sensor used to illustrate the efficiency of the proposed design flow is briefly discussed. The system-level block diagram, which consists of three major components, is shown in Fig. 3(a) [22].

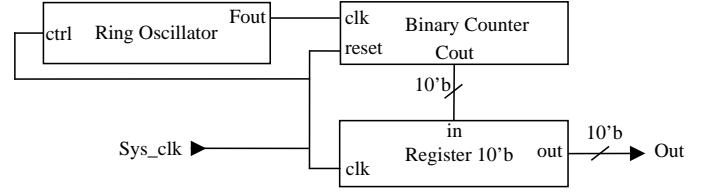
The 10-bit binary counter consists of JK flip-flops. The 10-bit register stores the value from the counter and is also implemented with JK flip-flops. The ring oscillator (RO) consists of a cascade of an odd number inverters connected in a loop. The RO used has 15 stages. The oscillation frequency is expressed as:

$$f_{osc} = \frac{1}{n(t_{pLH} + t_{pHL})}, \quad (10)$$

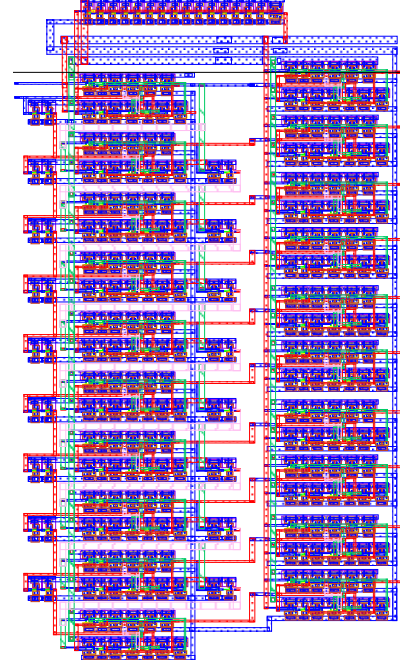
where  $n$  is the number of stages used in the oscillator and  $t_{pLH}$  and  $t_{pHL}$  are the low-to-high and high-to-low propagation delays respectively. In an ideal condition, the propagation delays can be expressed as [18]:

$$t_{pLH} = \frac{-2C_L V_{tp}}{\kappa_p (V_{dd} + V_{tp})^2} + \frac{C_L}{\kappa_p (V_{dd} + V_{tp})} \ln \frac{1.5V_{dd} + 2V_{tp}}{0.5V_{dd}}, \quad (11)$$

$$t_{pHL} = \frac{2C_L V_{tn}}{\kappa_n (V_{dd} - V_{tn})^2} + \frac{C_L}{\kappa_n (V_{dd} - V_{tn})} \ln \frac{1.5V_{dd} - 2V_{tn}}{0.5V_{dd}} \quad (12)$$



(a) Block Diagram.



(b) Physical design.

Fig. 3. Design of the proposed 45nm CMOS based thermal sensor.

where  $C_L$  is the capacitive load and  $\kappa_n$  and  $\kappa_p$  are the transconductance values given as:  $\kappa_{n/p} = \mu_n C_{ox} \left(\frac{W}{L}\right)_{n/p}$ . In Eqn. 10 - Eqn. 12, the threshold voltage  $V_t$  and mobility  $\mu$  are most sensitive to temperature and are given by [23]:

$$V_t(T) = V_t(T_0) + \alpha_{V_t}(T - T_0), \quad (13)$$

$$\mu(T) = \mu_0 \left(\frac{T}{T_0}\right)^{\alpha_\mu}, \quad (14)$$

where,  $\alpha_{V_t} = -0.5 - 3.0mV/^\circ K$  and  $\alpha_\mu = -1.2 - 2.0$ . An increase in temperature leads to an increase in the propagation delay which results in a decrease of the oscillating frequency.

The technology library used for the implementation of this thermal sensor is a 45 nm process design kit provided by Cadence. The thermal sensor design is characterized to sense temperatures between  $0^\circ C$  and  $100^\circ C$ . The  $Sys\_clk$  signal is used to enable the thermal sensor. When the  $Sys\_clk$  turns to logic zero, the ring oscillator is disabled, the counter is also reset and the register also stops saving the count, storing the last count value it had before the  $Sys\_clk$  was set to logic "0".

The binary counter is used to count the frequency difference between the ring oscillator output and the system clock. The count is stored in the 10-bit register and calibrated to measure the temperature change. The physical design of the thermal sensor is shown in Fig. 3(b).

The performance and accuracy of the physical design of the thermal sensor is degraded when compared to the schematic design. This is expected due to parasitic effects from the layout. A comparison between the schematic and physical design is presented in Table I. The power consumption is increased by 29%, from 293  $\mu\text{W}$  to 379.4  $\mu\text{W}$ . This circuit exhibits a linear dependence of oscillation frequency on junction temperature as shown in Fig. 4.

TABLE I  
THERMAL SENSOR OUTPUT COMPARISON.

Design	Average Power, ( $P_{TS}$ )	Sensitivity, ( $T_{TS}$ )	Area ( $\mu\text{m}^2$ )
Schematic	293.1 $\mu\text{W}$	16.88 MHz/ $^\circ\text{C}$	-
Layout	379.4 $\mu\text{W}$	9.42 MHz/ $^\circ\text{C}$	1221.37
% Change	29.44%	44.2%	-

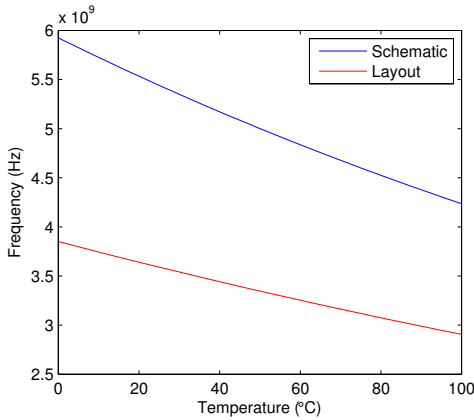


Fig. 4. Frequency response versus temperature for the thermal sensor.

The frequency response of the schematic design is 5.924 GHz (at 0 $^\circ\text{C}$ ) to 4.236 GHz (at 100 $^\circ\text{C}$ ). Assuming a 6 GHz max clock rate for the ring oscillator, and a 10 bit counter (1024 max count) the effective resolution is calculated by dividing the temperature range by the number count 100 $^\circ\text{C}/1024$  bit which gives a 0.097 $^\circ\text{C}/\text{bit}$  resolution. The range of frequency output is severely degraded by parasitics as seen in Fig. 4. The range drops to 3.867 GHz (0 $^\circ\text{C}$ ) and 2.986 GHz (100 $^\circ\text{C}$ ). There is a 47.8% change in frequency/temperature resolution by comparing the schematic design to the physical design. The area of the physical design is 1221.37  $\mu\text{m}^2$ .

## B. Results Analysis

In this section, the metamodel generation and the optimization results of the thermal sensor design are presented. For this design illustration, **six design parameters were chosen**, based on the 3 components of the thermal sensor. The widths of the NMOS and PMOS transistors in the RO are parameterized to

$WN_{osc}$  and  $WP_{osc}$ , respectively. The widths of the transistors for the 10-bit counter and 10-bit registers are parameterized to  $WN_{ctr}$ ,  $WP_{ctr}$ ,  $WN_{reg}$  and  $WP_{reg}$ , respectively. In generating the Kriging metamodels, 100 sample points were obtained from the LHS. To evaluate the accuracy of the generated metamodel, the metrics discussed in Section IV are used. The accuracy tests for MSE, RMSE and  $R^2$  metrics are shown in Table II.

TABLE II  
ACCURACY ANALYSIS OF THE SIMPLE KRIGING METAMODELS.

Metric	Value
$MSE$	$4.36 \times 10^{-18}$
$RMSE$	$2.09 \times 10^{-09}$
$R^2$	0.9934

From the results in Table II, the Kriging metamodels are sufficiently accurate with very low MSE and RMSE values of  $4.36 \times 10^{-18}$  and  $2.09 \times 10^{-09}$ . The correlation coefficient  $R^2$  is very close to 1 at 0.9934. The results validate the efficiency of Kriging metamodeling by producing very accurate metamodels while greatly reducing the simulation time required. The total time taken for the metamodel generation was approximately 30 hours, the bulk of this time being the simulation time required for the sample points. The time however is a factor of 10 lower than the approximately 300 hours required for an exhaustive simulation of the design.

In optimizing the thermal sensor, the GSA optimization is applied to the generated metamodel with an initial number of 50 search agents and a maximum iteration of 1000 runs. The design objective of the optimization is the minimization of power consumption. The results of the optimization run are shown in Fig. 5. From the optimization graph, it is seen that the algorithm is able to reach an optimized solution of 184.7  $\mu\text{W}$  in about 900 iterations.

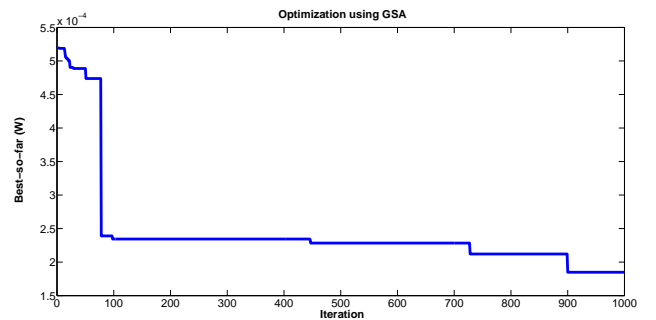


Fig. 5. GSA performance on Kriging metamodel for the 45 nm thermal sensor.

The final design parameters are shown in Table III. The final optimized FoMs of the thermal sensor are provided in Table IV. Comparing to the schematic baseline design, there is a 36.9% reduction in power dissipation. From the final design parameters, an area increase of about 45% is estimated, judging from the increase in transistor size.

TABLE III  
FINAL DESIGN PARAMETERS OBTAINED FROM THE KRIGING METAMODEL OPTIMIZATION.

Parameter	Value
$WN_{osc}$	215 nM
$WP_{osc}$	140 nM
$WN_{ctr}$	313 nM
$WP_{ctr}$	121 nM
$WN_{reg}$	224 nM
$WP_{reg}$	378 nM

TABLE IV  
THERMAL SENSOR OUTPUT COMPARISON

Design	Average Power, ( $P_{TS}$ )	Sensitivity, ( $T_{TS}$ )	Area ( $\mu m^2$ )
Schematic	293.1 $\mu W$	16.88 MHz/ $^{\circ}C$	-
Layout	379.4 $\mu W$	9.42 MHz/ $^{\circ}C$	1221.37
Final	184.7 $\mu W$	9.42 MHz/ $^{\circ}C$	1770.98*
% Change	36.9%	44.2%	45%*

## VIII. CONCLUSIONS

In this paper, a new design optimization flow incorporating a geostatistical inspired metamodeling technique (Kriging) and a gravitational search algorithm for analog/mixed signal circuits has been presented. The proposed methodology has been illustrated with the design optimization of a 45 nm thermal sensor design. Simple Kriging based metamodeling produces very accurate metamodels while reducing the time for exhaustive exploration of design space by about 90%. A total of six design parameters were considered for metamodeling and optimization. Thus, the proposed method is scalable to a large number parameters. The gravitational search algorithm also optimizes the design by reducing the power consumption by 36.9%. In future research, the metamodeling technique will be extended for process variation effects and statistical optimization.

## REFERENCES

- [1] W. E. Biles, J. P. C. Kleijnen, W. C. M. van Beers, and I. van Nieuwenhuysse, "Kriging Metamodeling in Constrained Simulation Optimization: An Explorative Study," in *Proceedings of the 39th Winter Simulation Conference*, 2007, pp. 355–362.
- [2] B. Ankenman, B. Nelson, and J. Staum, "Stochastic Kriging for Simulation Metamodeling," in *Proceedings of the Winter Simulation Conference*, Dec. 2008, pp. 362–370.
- [3] G. Dellino, J. Kleijnen, and C. Meloni, "Robust Simulation-Optimization using Metamodels," in *Proceedings of the Winter Simulation Conference (WSC)*, Dec. 2009, pp. 540–550.
- [4] O. Garitselov, S. Mohanty, E. Kougianos, and P. Patra, "Nano-CMOS Mixed-Signal Circuit Metamodeling Techniques: A Comparative Study," in *Proceedings of the International Symposium on Electronic System Design (ISED)*, 2010, pp. 191–196.
- [5] E. Rashedi, H. Nezamabadi-pour, and S. Saryzadi, "GSA: A Gravitational Search Algorithm," *Information Sciences*, vol. 179, no. 13, pp. 2232 – 2248, 2009.
- [6] T. Binder, C. Heitzinger, and S. Selberherr, "A Study on Global and Local Optimization Techniques for TCAD Analysis Tasks," *Computer-Aided Design of Integrated Circuits and Systems, IEEE Transactions on*, vol. 23, no. 6, pp. 814–822, June 2004.
- [7] V. Aggarwal, "Analog Circuit Optimization using Evolutionary Algorithms and Convex Optimization," Master's thesis, Massachusetts Institute of Technology, May 2007.

- [8] D. Lim, Y.-S. Ong, Y. Jin, and B. Sendhoff, "A Study on Metamodeling Techniques, Ensembles, and Multi-Surrogates in Evolutionary Computation," in *Proceedings of the 9th Annual Conference on Genetic and Evolutionary Computation*, ser. GECCO '07. New York, NY, USA: ACM, 2007, pp. 1288–1295.
- [9] G. G. Wang and S. Shan, "Review of Metamodeling Techniques in Support of Engineering Design Optimization," *Journal of Mechanical Design*, vol. 129, no. 4, pp. 370–380, 2007.
- [10] A. Khosravi, S. Nahavandi, and D. Creighton, "Developing Optimal Neural Network Metamodels Based on Prediction Intervals," in *International Joint Conference on Neural Networks*, June 2009, pp. 1583–1589.
- [11] R. A. Kilmer, A. E. Smith, and L. J. Shuman, "Computing Confidence Intervals for Stochastic Simulation Using Neural Network Metamodels," *Computers and Industrial Engineering*, vol. 36, no. 2, pp. 391–407, 1999.
- [12] H. You, M. Yang, D. Wang, and X. Jia, "Kriging Model Combined with Latin Hypercube Sampling for Surrogate Modeling of Analog Integrated Circuit Performance," in *Proceedings of the International Symposium on Quality of Electronic Design*, 2009, pp. 554–558.
- [13] G. Yu and P. Li, "Yield-Aware Analog Integrated Circuit Optimization Using Geostatistics Motivated Performance Modeling," in *Computer-Aided Design, 2007. ICCAD 2007. IEEE/ACM International Conference on*, Nov. 2007, pp. 464–469.
- [14] Y. Li and J. Li, "Swarm Intelligence Optimization Algorithm Based on Orthogonal Optimization," in *Computer Modeling and Simulation, 2010. ICCMS '10. Second International Conference on*, vol. 4, Jan. 2010, pp. 12–16.
- [15] O. Garitselov, S. Mohanty, E. Kougianos, and P. Patra, "Bee Colony Inspired Metamodeling Based Fast Optimization of a Nano-CMOS PLL," in *Electronic System Design (ISED), 2011 International Symposium on*, Dec. 2011, pp. 6–11.
- [16] B. Datta and W. Burleson, "Low-Power and Robust On-Chip Thermal Sensing Using Differential Ring Oscillators," in *Circuits and Systems, 2007. MWSCAS 2007. 50th Midwest Symposium on*, Aug. 2007, pp. 29–32.
- [17] Y. Zhang and A. Srivastava, "Accurate Temperature Estimation Using Noisy Thermal Sensors," in *Design Automation Conference, 2009. DAC '09. 46th ACM/IEEE*, July 2009, pp. 472–477.
- [18] T. Meng and C. Xu, "A Cross-Coupled-Structure-Based Temperature Sensor with Reduced Process Variation Sensitivity," *Semiconductors, Journal of*, vol. 30, no. 4, pp. 1642– 1648, Apr. 2009.
- [19] J. Sacks, W. J. Welch, T. J. Mitchell, and H. P. Wynn., "Design and Analysis of Computer Experiments." *Statistical Science*, vol. 4, no. 4, pp. 409–423, 1989.
- [20] G. Bohling, "Kriging," Kansas Geological Survey, Tech. Rep., 2005.
- [21] *mGstat: A Geostatistical Matlab Toolbox*. [Online]. Available: mgstat.sourceforge.net
- [22] S. Park, C. Min, and S.-H. Cho, "A 95nW Ring Oscillator-based Temperature Sensor for RFID Tags in 0.13  $\mu m$  CMOS," in *Circuits and Systems, 2009. ISCAS 2009. IEEE International Symposium on*, May 2009, pp. 1153–1156.
- [23] P. Chen, C.-C. Chen, C.-C. Tsai, and W.-F. Lu, "A Time-to-Digital-Converter-Based CMOS Smart Temperature Sensor," *Solid-State Circuits, IEEE Journal of*, vol. 40, no. 8, pp. 1642– 1648, Aug. 2005.